Airborne Observations of Contrail Effects on the Thermal Radiation Budget[1]

PETER M. KUHN

Atmospheric Physics and Chemistry Laboratory, ESSA, Boulder, Colo.

(Manuscript received 6 March 1970)

ABSTRACT

Direct infrared and solar radiometric observations were made to analyze the effects on the environment of any alterations in the radiation budget in regions of heavy jet traffic. The observations, made from the NASA Convair 990 jet laboratory, were coupled with Mie scattering and absorption theory calculations to analyze any inadvertent alterations in the natural atmospheric thermal radiation budget. It was found that a 500 m thick contrail sheet increases the infrared emission below the sheet by 21% but decreases the solar power below the sheet by 15%. The infrared increase cannot make up for the solar depletion, resulting in a net available incoming power depletion at the base of the sheet of 12%. Such a change at altitude results in a 7% reduction in the net total available thermal power at the earth's surface, which, in turn, results in a 5.3C decrease in the surface temperature, if we assume contrail persistence. The actual temperature decrease is ∼0.15C with 5% contrail persistence.

1. Introduction

Current well-directed, if not long overdue, interest in the environment of the earth concerns itself mainly with the biosphere. Pollution of the Great Lakes, rivers, streams and skies is an ever-present topic in a growing campaign that is only the prelude to widespread action.

Only beginning, however, is an increasing interest in the effects of inadvertent weather pollution. Yet the effects of such pollution from the surface to supersonic transport levels are basic to atmospheric changes. For it is in passing through our atmosphere that the thermal power budget of the biosphere is mainly determined, the budget that is our climate as we live in it today and as we may live in it tomorrow.

One aspect of weather pollution in the atmosphere is the generation of contrails. The spreading out of jet contrails into extensive cirrus sheets is a familiar sight. Often, when persistent conditions exist from 25,000 to 40,000 ft, several long contrails increase in number and gradually merge into an almost solid interlaced sheet. Since the possible effect of these tropospheric contrail sheets on the atmospheric thermal radiation budget is not clear, we have found it desirable to weigh the effects of increases in the infrared (IR) downward directed power against depletion in the solar power and have therefore undertaken extensive *in situ* radiometric research from the NASA jet aircraft laboratory on contrails and resulting cirriform sheets.

The Panel on Weather and Climate Modification (1966) discussed two possible effects of supersonic transport aircraft on the stratosphere—the possibility of a significant increase of stratospheric water vapor, and an increase in persistent cirriform cloud producing contrails. Both could affect the radiation budget and as a result possibly the general circulation. The Panel concluded that the addition of water vapor would not appreciably alter the radiation budget at the surface. The weight of water vapor released by supersonic jets operating at ∼60,000 ft is 40% greater than the weight of the fuel consumed. These conclusions were based on Manabe's[2] model calculations.

The Panel further concluded that with a total water vapor content in the stratosphere of about 2 ppm by mass (which in the light of recent reports in the literature appears a little too low) persistent contrails did not *appear* to be a hazard, because of the extreme dryness. This may be so. However, on our flights we have observed that non-persistent interlaced contrails influence the lower stratospheric and surface radiation budget for a relatively short time, which can result in atmospheric changes at lower levels. If we consider jet operations in the upper troposphere only, where saturation with ice occurs fairly frequently, the chances for persistence are higher than those in the stratosphere, and increasing tropospheric jet traffic may inject sufficient particulates into the upper troposphere to have a significant effect on the radiation budget in spite of the limited residence time of such pollutants.

[2] Manabe, S., 1965: Dependence of the climate on the change of the content of some atmospheric absorbers. Paper delivered before Panel on Weather and Climate Modification, Woods Hole, Mass.

FIG. 1. Morning contrails, Boulder, Colo.,
17 December 1969.

All our IR measurements above and below artificial cirrus displayed anomalous departures from simultaneous radiation calculations for a gaseous atmosphere. This suggests possibly simple additions to the radiative transfer equation to account for the additional radiation in thermal budget calculations. Zdunkowski *et al.* (1965), Zdunkowski and Choronenko (1969) and Hall (1968) have investigated a related problem, that of the effect of stratospheric haze on IR radiance and the blackness of clouds in the infrared.

Contrail development and spreading begins in the morning hours with the start of heavy jet traffic and may extend from horizon to horizon as the air traffic peaks. Fig. 1 is a typical example of midmorning contrails that occurred on 17 December 1969 northwest of Boulder. By midafternoon, sky conditions had developed into those shown in Fig. 2, an almost solid contrail sheet reported to average 500 m in depth.

Addressed directly to the question of the radiative effects of conventional and supersonic transport exhaust products, our research is aimed at determining, experimentally and by applied Mie absorption and scattering theory, the effects of contrails and contrail sheets on the atmospheric IR and solar thermal radiation budget and at reconciling calculations and observations. The investigations, currently conducted to 42,000 ft, will be extended to 65,000 ft within the year.

The research plan specifies the following objectives:

1) Observation of the IR transmissivity and scattering in the 10.0–12.0 μ spectral interval from flights over and under contrail sheets.

2) Observation of the upward, downard and reflected hemispheric solar radiant power from the aircraft platform.

3) Calculation by Mie theory of the IR transmissivity and scattering for monodispersed equivalent spherical ice particles of assumed 50 μ radii. This method is a modification of the one used by Zdunkowski *et al.* (1965), the main variable being the particle concentration.

4) Comparison of calculations of transmissivity and scattering with observations by iterating the radiative transfer solution on the particle concentration, the radiance and contrail depth being known.

5) Comparison of the calculated particle concentration for a number of samples with that assumed by Zdunkowski *et al.* (1965) and Hall (1968) for the same latitude.

6) Extension of results based on calculated IR transmissivities and scattering of the contrail sheets and observed solar reflectivity and transmissivity to determine changes in the available power at the level of the base of the contrail sheets and at the surface before and after formation; study of effects of infrared power augmentation and solar power depletion.

2. Instrumentation and observation procedure

All radiometric measurements were made from the NASA Ames Research Center Convair 990 jet laboratory over California and over the Atlantic east of Barbados.

A multichannel, narrow-field radiometer with a bolometer detector and 4-inch Cassegrainian fore-optics was the primary infrared instrumentation. Two hemispheric pyranometers responsive out to 2.5 μ measured the upward and downward solar irradiance. Radiometric measurements, time, altitude and auxiliary data were recorded every 2 sec.

The field of view of the IR radiometer is 0.14×0.14° (nominally 2.5 mrad). The effective solid angle aperture

TABLE 1. Radiometer transmissivity.

Wavenumber (cm^{-1})	Wavelength (μ)	Transmissivity
810	12.3	0.00
830	12.02	0.04
850	11.8	0.50
870	11.5	0.67
890	11.2	0.68
910	11.0	0.78
930	10.7	0.82
950	10.5	0.84
970	10.3	0.81
990	10.1	0.61
1010	9.9	0.13
1030	9.7	0.03
1040	9.6	0.00

is 13.9×10^{-6} ster. The noise equivalent radiance (NEN) is 3.08×10^{-7} mW cm^{-2} ster^{-1}. A single-channel filter recorded radiance in the 10.0-12.0 μ window. Table 1 gives the transmissivity of the filter. Pre- and post-flight calibrations were accomplished against a precision black cone cooled from 0C to -135C by liquid nitrogen.

For comparison of measurements with calculations of two-directional infrared radiant transfer through contrails and cirriform sheets, we required a model for the observed transmissivity and reflectivity of contrails, two basic nondimensional quantities. The simplified model used is given in Fig. 3. As shown here, the flight path made it possible to observe upward and downward radiance, $N\uparrow$ and $N\downarrow$, at the contrail or cirriform sheet base level "1" and at the top "2."

Downward radiance at level "1," for any spectral interval, is given by

$$N_1\downarrow = \tau_0 N_2\downarrow + \rho_0 N_1\uparrow + (1-\tau_0-\rho_0)N_c, \qquad (1)$$

where τ_0 is the observed contrail or cloud transmissivity, ρ_0 the reflectivity, and N_c the cloud IR radiance at the mean cloud temperature. The transmissivity then follows from (1), i.e.,

$$\tau_0 = (N_1\downarrow - N_c - \rho_0 N_1\uparrow)/(N_2\downarrow - N_c). \qquad (2)$$

Similarly, the upward radiance and cloud transmissivity at level "2" are given by

$$N_2\uparrow = \tau_0 N_1\uparrow + (1-\tau_0)N_c, \qquad (3)$$

$$\tau_0 = (N_2\uparrow - N_c)/(N_1\uparrow - N_c). \qquad (4)$$

In all instances the radiances are observed quantities.

Combining (2) and (4), we obtain for the contrail or cloud IR reflectivity

$$\begin{aligned} \rho_0 = [&- (N_2\downarrow - N_c)(N_2\uparrow - N_c) \\ &+ (N_1\downarrow - N_c)(N_1\uparrow - N_c)]/ \\ &\qquad\qquad [N_1\uparrow(N_1\uparrow - N_c)]. \end{aligned} \qquad (5)$$

Upward and downward hemispheric fluxes were obtained from temperature-compensated aircraft-type pyranometers on flights above and below the contrail sheets. The high speed and climbing rate of the jet aircraft eliminated any large time lapse between observations of downward and upward propagating solar power. The pyranometers exhibited a 1.5% random error and were calibrated before and after flight against an Angstrom pyranometer.[3]

3. Transmissivity and scattering calculations

In discussing radiance from cirrus clouds, and cloud transmissivity and reflectivity, we must define the optical properties of such clouds. The size of the contrail ice crystals, the optical constants of ice, and the

---

[3] Pyranometer results were by courtesy of A. J. Drummond and J. R. Hickey, Eppley Laboratories, Newport, R. I.
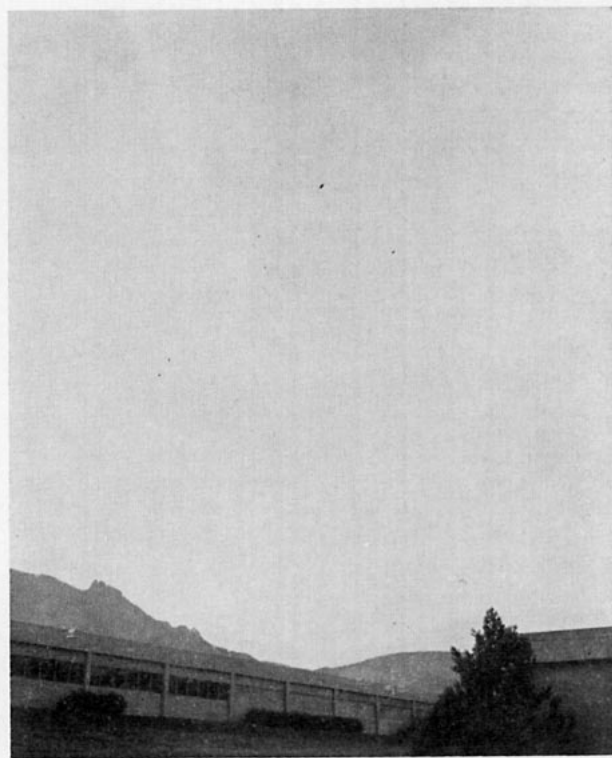

FIG. 2. Afternoon contrail sheets, Boulder, Colo., 17 December 1969.

optical thickness of the layer must be known. The size parameter α, equal to $2\pi r/\lambda$, where r is the particle radius and λ the wavelength, derives from these properties. Later comparisons will require reference to this parameter. The efficiency factors for extinction, absorption and scattering, Q_{ext}, Q_{abs}, Q_{sca}, were calculated by Barrett's (1970) method. A value of $1.38-0.35i$ for the complex index of refraction of ice in the 6.0–50.0 μ region (Kislovskii, 1959) was adopted for the computations. The final values for the efficiency factors for ice, shown in Fig. 4, agreed with those calculated by Twomey (1963).

Weickmann (1949) completed an extraordinary comprehensive study of the physical properties of cirrus clouds, based on cirrus particles collected on coated glass slides from an aircraft open cockpit at altitudes up to 32,500 ft. He demonstrated that the most typical cirrus particle is a hollow prism, 30.0 μ by 200.0 μ, and showed that the equivalent solid ice sphere would have a radius of 38.0 μ. A hollow equivalent sphere of twice this volume can be shown to have a radius of 50.0 μ, a
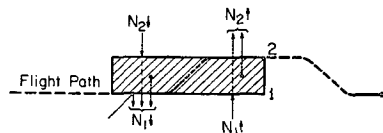

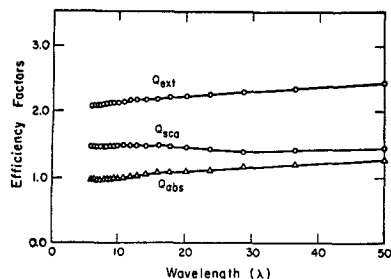FIG. 3. Model of observed cirriform type cloud radiation budget.

FIG. 4. Mie efficiency factors for 50.0 μ
radius ice particles.

configuration adopted in this work as representative of the average monodispersed ice crystal.

Calculations of the Q factors just discussed were made for 50.0 μ particles. Fig. 4 illustrates that at wavelengths from 6.0–50.0 μ these parameters vary little. Mie theory calculations indicate that for a size parameter α as large as 31.0, one-half of the power will be within a 1.4° scattering angle from the source. Thus, an extinction efficiency of $\sim$1.0 should be used in calculations of the effective cross section for extinction, absorption and scattering (Hall, 1968).

Subsequent computations require a knowledge of the effective cross sections for extinction, absorption and scattering. These are defined by

$$C_{ext} = \pi r^2 Q_{ext}, \tag{6}$$

$$C_{abs} = \pi r^2 Q_{abs}, \tag{7}$$

$$C_{sca} = \pi r^2 Q_{sca}, \tag{8}$$

where πr^2 is the geometric cross section of the particle. Note that

$$Q_{ext} = Q_{sca} + Q_{abs}. \tag{9}$$

It is also clear that

$$C_{ext} = C_{abs} + C_{sca}, \tag{10}$$

and we term C_{ext} the total extinction coefficient.

With a particle radius of 50.0 μ for the equivalent hollow ice sphere, (6) gives 0.865×10^{-4} cm^2 for the

effective cross section for extinction or the total extinction coefficient, including absorption and scattering.

Zdunkowski *et al.* (1965) and Hall (1968) investigated by calculations and ground-based observations, respectively, the influence of thin cirrus layers on IR radiant emittance leaving the atmosphere. Zdunkowski assumed equivalent spheres of 120.0 μ radii, while Hall assumed spheres of 50.0 μ radii based on Weickmann's (1949) research. On the assumption that these spherical ice particles act as primary scatterers and absorbers of IR radiation, they developed a radiative transfer solution for radiative propagation through an ice cyrstal medium. The author followed the same general method in developing calculations for transmissivity and scattering for assumed equivalent 50.0 μ ice spheres from Mie theory. It can be shown that a change in the equivalent sphere radius would merely change the particle concentration N (cm^{-3}).

If we assume that the emission spectrum of the ice particles is essentially continuous, and this is not a gross assumption, the sum of the calculated transmissivity τ_c and reflectivity ρ_0 is

$$\tau_c + \rho_0 = \exp(-C_{ext} M \sec\theta), \tag{11}$$

where M (cm^{-2}) is the attenuating mass given by $\Sigma_i N(\Delta\zeta)_i$, $\Delta\zeta$ an increment of depth in centimeters, and θ the zenith angle, set equal to zero for our purposes.

At this point it was necessary to iterate through several calculations of (11) to minimize the quantity $|\Sigma(\tau_0 - \tau_c)^2|$. This was accomplished by holding all terms in (11) constant except M. Since the depth of the contrail sheet, $\Delta\zeta$, is known, the only variable is the particle concentration N. The iteration was carried out on N. Measurements were made on 11 and 17 June 1968 between 35,000 and 40,000 ft over California and in 1969 at the same altitudes in the Barbados, West Indies, region. Ten individual passes over and under contrail sheets were made. As measured later (1969) by lidar the mean thickness of the contrail sheets was 500 m. Each pass, lasting from 30–60 sec, provided a complete set of observations of all required parameters every 6 sec. Table 2 lists the averages of observed radiances

TABLE 2. Observed contrail effects on radiation parameters.

Radiation parameter	Observed (10⁻⁴ W m⁻² ster⁻¹)	Standard deviation (10⁻⁴ W m⁻² ster⁻¹)	Standard error (10⁻⁴ W m⁻² ster⁻¹)	Observed (percent)	Calculated (percent)	Calculated $\nearrow$ (cm⁻³)
$N_1\downarrow$	0.961	0.012	0.004			
$N_1\uparrow$	22.748	2.010	0.670			
$N_2\downarrow$	0.287	0.025	0.009			
$N_2\uparrow$	20.814	1.873	0.624			
N_c	4.700	7.050	2.350			
τ_0	—	—	—	0.890	0.893	
ρ_0	—	—	—	0.006	0.009	
α'	—	—	—	0.150±0.017		
N	—	—	—	—	—	0.027

α' is the hemispheric solar albedo.

for the ten contrail passes, the calculated mean of the various radiances, the observed and calculated transmissivity and reflectivity of the means, and the particle concentration calculated from the same means. Because of the NEN (noise equivalent radiance) of the radiometer, 3.08×10^{-7} mW cm^{-2} ster^{-1}, three significant decimals are tabulated for the radiances.

4. Analyses of results

In solving (11) for the particle concentration N, we used the observed transmissivity and reflectivity [Eqs. (2), (4) and (5)], an equivalent sphere radius for the ice crystals of 50.0 μ, and a measured contrail depth, $\Delta\zeta$. The particle concentration obtained, 0.027 cm^{-3}, is , as Table 3 shows, quite compatible with those reported by other researchers.

One might well expect a particle concentration somewhat less for contrails than for natural cirrus. Any change in the particle radius in (11) would merely change the particle concentration to satisfy the solution. Thus, a transmissivity τ_0 of 0.90 and reflectivity ρ_0 of 0.01, as observed, was used in the radiative transfer calculations to be considered.

The results suggest a simple addition to the mathematical formulation for the radiant power transfer received by a perfect detector, i.e.,

$$N(P_0,\theta)\downarrow = -\int_{\lambda_1}^{\lambda_2}\int_{p=0}^{p_0} B[\lambda, T(p)]\frac{\partial}{\partial p}[\tau_0(\lambda,T,U,p)]dp\,d\lambda$$
$$-\int_{\lambda_1}^{\lambda_2}\int_{p=0}^{p_0} B[\lambda, T(p)]\frac{\partial}{\partial p}[\tau_0(M)]dp\,d\lambda. \quad (12)$$

Here B is the Planck function, T the absolute temperature, p the pressure, U the optical depth of the radiating atmospheric gases, and λ the wavelength. The addition for the ice particle emission is in the second term on the right. In this simple model formulated by the second term of (12), τ_0 is the assumed constant between λ_1 and λ_2 and is independent of pressure broadening and temperature effects. It is thus possible to apply (12) to a direct solution of radiant power transfer in the presence of ice crystals over the 3.5–40.0 μ "total" spectral region. We use the transmissivity and reflectivity over this region as observed over the 10.0 12.0 μ interval. This is possible since the efficiency factors and Mie cross sections are essentially constant from 5.9 μ through 50.0 μ (Fig. 4). We can now assess the net effect of downward IR power increase caused by the contrails and solar power decrease.

Eq. (12) was solved for the downward radiant emittance (ly day^{-1}), with the sounding data obtained from the ESSA Coast and Geodetic Survey oceanographic vessel *Discoverer* on 9 June 1969 at 13N, 53W. The purpose of the calculations was to determine the power depletion caused by contrail sheets in, first, a tropical atmosphere and then in a continental atmosphere. Fig.
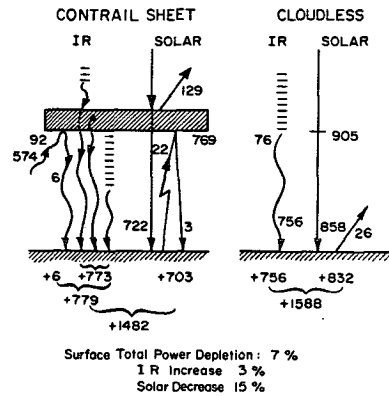

Fig. 5. Tropical radiation budget, cloudless and beneath contrails.

5 illustrates the results under cloudless and contrail sheet conditions. The units are langleys per day (cal cm^{-2} day^{-1}) to provide the complete daily budget. The solar input at contrail and surface levels is based on comparison of observed data with calculations by Barrett (1970). The total daily infrared plus solar power depletion in the presence of interlaced contrail sheets for this tropical sounding is 7% at the surface. Clearly the depletion of solar power caused by the observed 15% albedo of the contrail exceeds the 21% increase in the downward IR power resulting from the contrail. If we assume radiative equilibrium and the ocean surface to be an infinite black source at 25C, the temperature decrease would be 5.3C for persistent contrails.

For comparison, Fig. 6 illustrates the radiant power depletion and budget calculations from a solution of (12) based on mean cloudless sounding data (pressure, temperature and humidity) for Washington, D. C., for the month of June (5 year mean sounding). The total surface power depletion is 8% in the presence of contrail sheets, slightly higher than in the tropics. However, the continental time constant would be much shorter than the oceanic climate response, and the power depletion would result in a 6.0C temperature fall, if we assume surface radiative equilibrium with an infinite black

TABLE 3. Cirrus type cloud ice particle concentration.

Researcher	Method	Cloud depth (km)	Concentration (cm^{-3})
Weickmann	Aircraft visual observations		0.050
Hall	Inference from surface radiometric observations	0.2	0.050
Zdunkowski*	Calculations related to radiometric balloon observations	1.0	0.002
This study	Inference from *in situ* aircraft radiometric observations	0.5	0.027

* Zdunkowski (1965) considered only an "invisible" cirrus haze, stating that the visual threshold for cirrus occurs at a particle concentration of 0.0015 cm^{-3}.
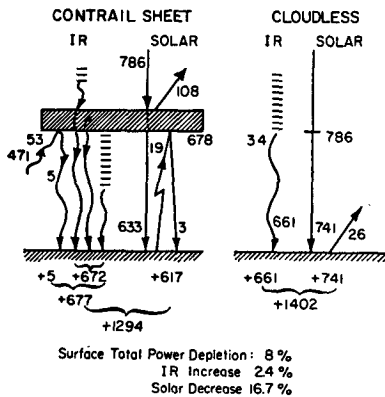
FIG. 6. Mid-latitude radiation budget, cloudless and beneath contrails.

ground source at 18C. Again, contrail persistence is assumed. With a contrail persistence of only 5% over a long term, the power depletions for Figs. 5 and 6 would be 0.35 and 0.4%, respectively. The corresponding temperature falls would be 0.3C and 0.3C, respectively— still significant. If we further speculate that deeper cloud cover would occur on one out of every three days in both cases and that it would mask contrail effects, the temperature falls would be 0.15C and 0.15C.

5. Summary

The particle concentration of contrail sheets composed of assumed monodispersed equivalent hollow spherical ice particles, derived from radiometric theory, is consistent with a derivation of the same quantity from *in situ* radiometric observations of contrails. The contrail sheets observed from NASA's Convair 990 jet laboratory averaged 500 m in depth and increased in IR radiant emittance by 21% beneath the contrail but decreased the solar power by 15%. This results in a net depletion of 12% at the contrail base. The surface power depletion is 7% for the tropics and 8% for continental summer conditions, if we assume 100% persistence. The

thermal budget in this instance is controlled by the solar power depletion. More realistically, on the assumption of a maximum 5% contrail persistence and 33% cloud cover on an annual basis, the total available surface power depletion would be approximately 0.12%, resulting in a temperature drop at the surface of only 0.15C.

If stratospheric, or for that matter upper tropospheric, conditions would be suitable for 5% contrail persistence (i.e., saturation with ice), then we have shown that the loss in available radiant power at the surface would result in only slight surface cooling. This would not cause general changes in the planetary circulation or the length of the growing season. In fact, beyond the immediate vicinity of a contrail overcast, climatic effects of thermal budget modifications rapidly diminish. One can speculate that ultimately so many jets may be operating in certain high density corridors that contrail persistence of 10% will occur, with possible local transistory alterations in the circulation.

REFERENCES

Barrett, E. W., 1970: Comments on ESSA-APCL Mie backscattering programs. ESSA Research Laboratories, Boulder, Colo., 10 pp.

Hall, F., 1968: The effect of cirrus clouds on 8–13 μ infrared sky radiance. *Appl. Opt.*, **7**, 891–898.

Kislovskii, L. D., 1959: Optical characteristics of water and ice in the infrared and radiowave regions of the spectrum. *Opt. Spectry.*, **3**, 201–206.

Panel on Weather and Climate Modification, 1966: *Weather and Climate Modification: Problems and Prospects.* Publ. No. 1350, Washington, D. C., National Academy of Sciences–National Research Council, 198 pp.

Twomey, S., 1963: Tables of scattering and extinction efficiencies for complex refractive indices. Unpubl. Rept., Weather Bureau, Physical Science Laboratory, Washington, D. C.

Weickmann, H. K., 1949: Die Eisphase in der Atmosphare. *Ber. Deut. Wetterdiensts*, U. S. Zone, Germany, No. 6.

Zdunkowski, W., and I. Choronenko, 1969: Incomplete blackness of clouds in the infrared spectrum. *Beitr. Phys. Atmos.*, **42**, 206–223.

——, D. Henderson and J. V. Hales, 1965: The influence of haze on infrared radiation measurements detected by space vehicles. *Tellus*, **17**, 147–165.